

RESEARCH

Open Access



# Alleviating penicillin-resistant *Streptococcus pneumoniae*-induced lung epithelial cell injury: mechanistic insights into effects of the optimized combination of main components from Yinhuapinggan granules

Jiangbo Lv<sup>1,2†</sup>, Haofang Wan<sup>1,2†</sup>, Daojun Yu<sup>3\*</sup>, Huifen Zhou<sup>1,2</sup>, Wenba Wang<sup>1,2</sup> and Haitong Wan<sup>1,2,4\*</sup>

## Abstract

**Objective** Penicillin-resistant *Streptococcus pneumoniae* (PRSP), for which novel treatment medicines are required, has expanded extensively due to the overuse of antibiotics. This study aimed to detect the optimal ratio of the combination of the main components based on Yinhuapinggan granules (YHPG) to generate novel treatment concepts for PRSP-induced lung injury.

**Methods** Three representative main components: chlorogenic acid (C), amygdalin (A), and puerarin (P) were selected, and the optimal combination of these three components was determined by an orthogonal experiment. Investigations were conducted on the potential mechanisms underlying the protective effect of this optimized combination against PRSP-induced lung epithelial cell damage. Meanwhile, the bacteriostatic effect was further explored through the optimized combination of these natural products combined with penicillin G (PG).

**Results** The optimized combination CAP (C: 16 µg/mL, A: 24 µg/mL, P: 24 µg/mL) screened by the orthogonal experimental design reduced cell damage in a model of human lung epithelial cells infected by PRSP, and the combination of CAP and PG had a synergistic effect. At the cellular level, CAP attenuated lung epithelial cell injury by modulating the TLRs/MyD88 inflammatory pathway. At the bacterial level, CAP modulated the virulence and drug resistance of PRSP, resulting in enhanced bacterial inhibition by the combination of CAP and PG.

**Conclusion** Taken together, our results suggest that CAP can modulate or synergize with PG to modulate the TLRs/MyD88 pathway and attenuate PRSP-induced lung injury, and can be used as a potential drug for treating PRSP infection.

<sup>†</sup>Jiangbo Lv and Haofang Wan contributed equally to this work and share first authorship.

\*Correspondence:

Daojun Yu  
yudaojun98@163.com  
Haitong Wan  
whtong@126.com

Full list of author information is available at the end of the article



**Keywords** *Streptococcus pneumoniae*, Drug resistance, Lung injury, Inflammation, Yinhuapinggan granules

## Introduction

*Streptococcus pneumoniae* (SP) is a major worldwide pathogen producing pneumonia, sepsis, and meningitis [1]. SP pneumonia is the primary cause of lower respiratory tract infections globally, causing over a million fatalities each year [2].  $\beta$ -lactam antibiotics, represented by PG, are the first-line treatment for SP disease [3]. However, the effectiveness of PG therapy is being called into question because of the worrying increase and spread of antimicrobial resistance among SP isolates as a result of antibiotic abuse [4]. The World Health Organization (WHO) has included PRSP among the drug-resistant bacteria for which there is an urgent need for new antibiotics [5]. Therefore, there is a need to find new drug candidates or potential therapies to combat pneumonia caused by PRSP [6].

To seek alternative solutions to the problem of drug-resistant bacteria, researchers have made many attempts, such as anti-infective compounds that can directly target pathogen-specific virulence factors [7], artificial nanomaterials that can be targeted to break the physiological response within the pathogenic bacteria [8], or novel antibiotics with low clinical side effects [9]. In contrast, traditional Chinese medicine components, especially botanical components, have the advantages of high safety, environmental sustainability, and diversified antibacterial mechanisms, and can circumvent the substantial investment and time required to develop novel drugs [10]. Compounding of botanical drugs has antibacterial and antiviral potential [11], and herbal components often demonstrate the advantages of being less prone to resistance to pharmaceuticals in the management of bacterial pneumonia [12]. For instance, Ma-xing-shi-gan-tang [13] can diminish the virulence of the bacterium in an infection study involving SP, while Xuanfei Baidu Decoction [14] has beneficial impacts on lipopolysaccharide (LPS)-induced acute pulmonary damage.

YHPG consists of *Puerariae lobatae radix*, *Lonicerae japonicae flos*, *Polygoni cuspidati rhizoma et radix*, *Ephedrae herba*, *Armeniacae semen amarum*, and *Glycyrrhizae radix et rhizoma* in a mass ratio of 4:4:4:2:2:1 [15]. The formulation has good efficacy in relieving cough, promoting lung relief and removing heat and toxins [16]. During our prior study, we discovered that YHPG was able to reduce the inflammatory response [15] of the lungs induced by influenza virus and lessen lung damage [17] from multidrug-resistant *Acinetobacter baumannii*.

Toll-like receptors (TLRs) are key pattern recognition receptors (PRRs) in the human body during the process of undergoing microbial infections and are often considered suitable targets for the regulation of innate

immunity [18]. The sustained activation of the TLRs signaling pathway leads to the aberrant activity of transcription factors such as NF- $\kappa$ B and IRF [19], which triggers a burst of cytokine (e.g., IL-6, TNF- $\alpha$ , IFN) release. The inflammatory process in the alveolar tissues of patients with severe infectious pneumonia results from the “cytokine storm”. Therefore, inhibition of overexpressed TLRs seems to be a solution to counteract the cytokine storm [20]. Previous studies have shown that YHPG attenuates the inflammatory response in influenza virus (IFV)-infected mice by down-regulating TLR4 [21] and reduces the expression of TLR7 in Madin Darby canine kidney (MDCK) cells in the viral-infected MDCK model [12].

However, Chinese compounding of botanical drugs often contains complex components, and the exact mechanism of its efficacy is unclear [22]. Therefore, we selected the three main components of YHPG, C, A, and P, in this study and optimized the ratios of these three components through an orthogonal design to determine the optimal combination of them for PRSP inhibition. In addition, many evidences show that the antibacterial impact of using both herbal components and antibiotics together is enhanced [23], outperforming the usage of either component alone. For example, it was shown [24] that Glabrol, a natural flavonoid component from plants, showed synergistic antibacterial activity with colistin by promoting membrane disruption in Gram-negative bacteria. In another study [10], Baicalein can reverse the resistance of MRSA to ciprofloxacin by inhibiting the Nora efflux pump in vitro, thus realizing synergistic antibacterial activity with ciprofloxacin. Based on this concept, we used the optimized combination of YHPG natural products alone or in combination with PG at the same time to investigate the protective effects and its possible mechanisms based upon the PRSP-induced human pulmonary epithelial cell model.

In this study (Fig. 1), for the characteristics of traditional Chinese medicine compound YHPG with broad spectrum but dispersed efficacy [12, 15, 17, 21], we focused on the synergistic treatment of targeting drug-resistant bacterial characteristics and immune microenvironment modulation through the optimized combination, CAP, to fill the gaps of natural medicines in synergizing the antimicrobial mechanism with the mechanism of attenuating cell damage.

## Materials and methods

### Bacterial isolates and cells

The SP strains utilized in this investigation were isolated from the Clinical Laboratory, Hangzhou First People's Hospital. The bacteria were incubated at 37°C in 5% CO<sub>2</sub>

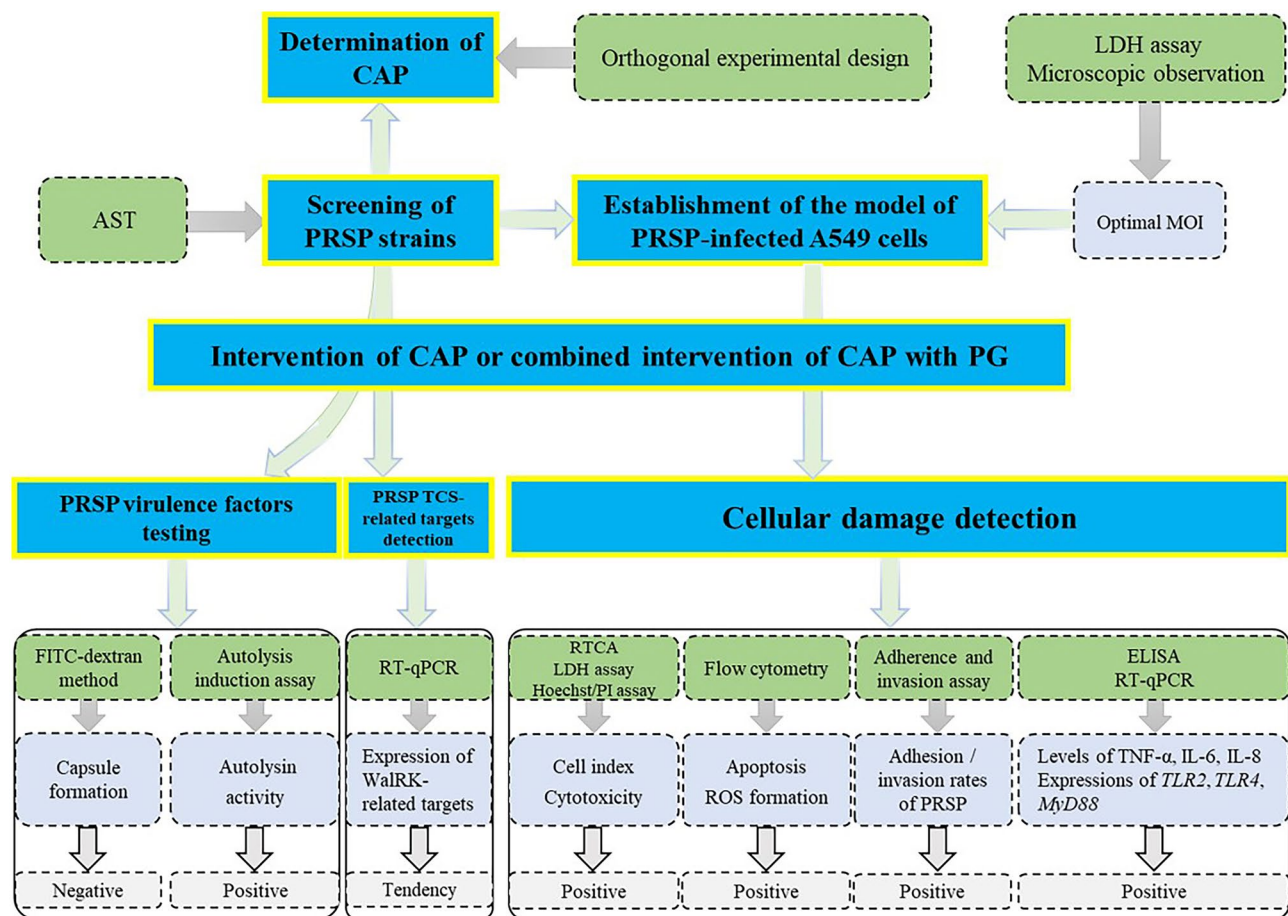


**Fig. 1** The experimental flowchart of this study, including the corresponding main experimental methods and experimental results

with shaking at 200 RPM. A549 cells were chosen for the investigation since they are a common in vitro model for evaluating lung injury [25]. A549 cells were passaged in F-12 K medium (Boster, Wuhan, China) containing 10% fetal bovine serum (FBS, GIBCO, Brazil) and 100 U/mL penicillin-streptomycin solution (Beyotime, Shanghai, China) at 37°C and 5% CO<sub>2</sub>. The cell line was kept in our laboratory. All isolates and cells were stored at -80°C.

### Reagents

Chlorogenic acid (C, ≥98%, Lot No. AF21012553), amygdalin (A, ≥98%, Lot No. AF20070652), and puerarin (P, ≥98%, Lot No. AF20023001) were obtained from Chengdu Alfa Biotechnology Co., Ltd. (Chengdu, China). Penicillin G potassium salt and vancomycin were purchased from Shanghai Aladdin Biochemical Technology Co., Ltd. (Shanghai, China).

The enzyme-linked immunosorbent assay (ELISA) kits for tumor necrosis factor-alpha (TNF-α), interleukin-6 (IL-6), and interleukin-1 beta (IL-1β) were purchased from Jiangsu Meibiao Biotechnology Co., Ltd. (Yancheng, China). Lactate dehydrogenase (LDH) Assay Kit and Annexin V-fluorescein isothiocyanate (FITC) Apoptosis

Kit were provided by Beyotime Biotechnology Co., Ltd. (Shanghai, China).

### Antibiotic susceptibility test (AST)

PG, C, A, and P were dissolved in MH broth and filtered using 0.22 μm membrane filters. The drug solutions were separately diluted in multiplicity in 96-well plates using MH broth. The overnight cultured suspension was inoculated into 96-well plates containing antimicrobial drugs and MH broth so that the culture was diluted to 10<sup>6</sup> colony forming units (CFUs)/mL and incubated as described above. The inhibition of SP strains by PG, C, A, and P was detected by the broth microdilution method according to the standards recommended by the Clinical and Laboratory Standards Institute (CLSI).

### Determination of maximal atoxic concentration (TC0)

A549 cells were added to 96-well plates (2 × 10<sup>3</sup> cells/well) with varying amounts of C, A, and P, while a control group without drugs was established. The final volume of each well reached 100 μL. Following a 24-hour culture at 37 °C and 5% CO<sub>2</sub>, the effects of drugs on the

**Table 1** Three-factor and three-level of orthogonal experiment

Factor Level	C( $\mu\text{g/mL}$ )	A( $\mu\text{g/mL}$ )	P( $\mu\text{g/mL}$ )
1	4	24	24
2	8	48	48
3	16	96	96

**Table 2** Arrangement of orthogonal experiment

Group	C	A	P
A	1	1	1
B	1	2	2
C	1	3	3
D	2	1	2
E	2	2	3
F	2	3	1
G	3	1	3
H	3	2	1
I	3	3	2

proliferation of A549 cells were measured using the Cell Counting Kit-8 (CCK-8, Beyotime, Shanghai, China).

#### Orthogonal experimental design

The orthogonal experiment was conducted to determine the optimal ratios of the three main components (C, A, and P) of the botanical formulation YHPG. All three components were set into three doses at low, medium, and high levels, and the specific dose settings (Table 1) and group settings (Table 2) were as follows. The culture was diluted to around  $10^6$  CFUs/mL by adding SP suspensions in the logarithmic growth phase to medium containing the combinations of these three natural medicines. In contrast to the experimental group, the control group did not receive any pharmacological additions. The OD600 was measured after each group was cultured to the logarithmic growth stage, from which the inhibition rate of each experimental group relative to the control group was calculated.

#### PRSP infection

A549 cells were inoculated in cell culture plates with single wells containing F-12 K medium supplemented with 10% FBS and 2% penicillin-streptomycin. After the cell fusion reached 90%, the cells were given three phosphate-buffered saline (PBS) washes before being added to each well with F-12 K and FBS free of antibiotics. At the same time, PRSP was added to each well to infect the cells with varying multiplicity of infection (MOI).

The infection of different MOIs was analyzed by microscopic observation (cells in 96-well plates) and LDH assay (cells in 6-well plates) after 12 h, from which the best MOI for bacterial infection of A549 cells was selected. The subsequent models of PRSP infection of A549 cells were performed according to this operation and in 6-well plates, unless otherwise specified.

#### Bacterial virulence factors or TCS-related targets testing

The capsule of PRSP was measured by the FITC-dextran method. 10  $\mu\text{L}$  of PRSP suspension in the logarithmic growth phase was aspirated and 2  $\mu\text{L}$  of FITC-dextran FITC-dextran (10 mg/mL, MedChemExpress, NJ, USA) was added. The mixture was dripped onto a slide and sealed tightly with a cover slip and placed on a confocal laser scanning microscope (CLSM) for observation with a 63 $\times$  objective.

PRSP autolysin activity was assayed by the autolysis induction assay. A portion of PRSP bacterial suspensions at mid-logarithmic growth was taken, centrifuged (12,000 rpm, 5 min), and resuspended in PBS with 0.5% Triton X-100 (Aladdin, Shanghai, China). PBS alone without Triton X-100 was also used as a control (PBS group). Following that, these suspensions were incubated at 37  $^{\circ}\text{C}$ . A reduction in OD600 with time was defined as PRSP lysis. The results were expressed as a percentage, which was computed by dividing the observed OD600 by the original OD600.

PRSP *WalR* TCS-related targets were detected by RT-qPCR. For each group, 5 mL of logarithmic growth phase bacterial cultures were taken, and the bacterial fluids were centrifuged and cleaned twice with PBS, then resuspended using the TRIzol reagent, and the extraction of the total RNA was initiated. The corresponding cDNAs were subsequently prepared according to the Reverse Transcription Kit (Biosharp, Hefei, China), and the final amplification was performed using Universal SYBR qPCR Master Mix (Biosharp, Hefei, China). The relative expression of target genes (*WalR*, *Walk*, *StkP*, *PcsB*, *PspA*, *LytB*) was normalized using 16S rDNA as the internal reference gene and characterized by the 2- $\Delta\Delta\text{Ct}$  method.

#### Real time cellular analysis (RTCA)

A549 cells were seeded ( $1 \times 10^4$  cells/well) with F-12 K media (containing serum) in 16-well E-plates (xCELLigence, ACEA biosciences, San Diego, CA). Cell line behavior was recorded in real time using RTCA S16 Instrument (ACEA Biosciences Inc., San Diego, CA) for a continuous period of 48 h, during which time the cell index (CI) was monitored at a frequency of every 5 min. 24 h after inoculation, PRSP was added in accordance with the ideal MOI, and pharmacological treatments were carried out concurrently in the experimental group.

#### Cell damage detection

PRSP and A549 cells were co-cultured according to the optimal MOI. Drugs were introduced concurrently with the addition of the PRSP bacterial suspension. After 12 h of treatment, the protective effect of each group of drugs on A549 cells was assessed by LDH level. Another portion of cells was taken and after being treated in the same way, they were stained using Hoechst 33,342/PI Double

Stain Kit (Solarbio, Beijing, China) and observed with a fluorescence inverted microscope.

### Flow cytometry

After 12 h of treatment with PRSP and drugs, A549 cells were harvested using 0.25% trypsin solution, and the supernatant was collected. After being exposed to fluorescent probes, the cells were examined.

Apoptosis was detected using the apoptosis detection kit.  $2 \times 10^5$  cells from each group were taken into centrifuge tubes and resuspended with 200  $\mu$ L of binding buffer. Following the addition of 5  $\mu$ L of Annexin V-FITC and 10  $\mu$ L of propidium iodide (PI) staining solution, the mixture was incubated for 15 min at room temperature and away from light.

Intracellular reactive oxygen species (ROS) levels were detected using the ROS Assay Kit (Biosharp, Hefei, China). After centrifuging  $1 \times 10^5$  cells from each collection, the cells were resuspended in serum-free F-12 K medium containing 2',7'-Dichlorodihydrofluorescein Diacetate (HDCF-DA) probe. Then, the cells were incubated at 37 °C in a cell culture incubator for 30 min.

### Adherence and invasion assay

The cell-surface hydrophobicity (CSH) of PRSP was detected by the microbial adhesion to hydrocarbon (MATH) method. 2 mL of SP bacterial suspension (about  $10^8$  CFUs/mL) in logarithmic growth phase was co-cultured with 2 mL of drug solution for 24 h (group setup as above), and 0.8 mL of n-hexadecane (Yuanye, Shanghai, China) was added as the organic phase. After shaking for

60 s and standing for 15 min, 3.0 mL of the lower aqueous phase solution was quickly aspirated using a sterile syringe needle, and the absorbance was measured at 600 nm. 0.8 mL of PBS (instead of n-hexadecane) was added to the control group accordingly. The CSH of PRSP was calculated according to the following formula:

$$\text{CSH}(\%) = \frac{\text{OD600}(\text{control}) - \text{OD600}(\text{experiment})}{\text{OD600}(\text{control})} \times 100\%$$

Adhesion assay. A549 cells received treatment with PRSP and drugs for 12 h. The PRSP that did not adhere to the surface of the A549 cells was removed by rinsing them with PBS buffer. The cells were lysed for 10 min after 400  $\mu$ L of 0.5% Triton X-100 and 100  $\mu$ L of 0.25% trypsin solution were added to each well. The cell lysate was collected and diluted with PBS. 100  $\mu$ L of diluent was taken and was coated and separated upon culture plates. The colonies of each group were counted following a 16-hour incubation period.

Similar to the adhesion assay, the invasion assay involved incubating cells in F-12 K media containing 10  $\mu$ g/mL vancomycin for two hours prior to lysis in order to eliminate PRSPs that failed to invade A549 cells. In addition, the invasion of A549 cells by PRSP was observed using CLSM, and the nuclei of A549 cells were labeled with 4',6-Diamidino-2-Phenylindole (DAPI), as visualized by bright-field and DAPI fluorescence channels.

### Detection of inflammation-related indicators

Following a 12-hour co-cultivation of A549 cells with PRSP, the supernatants from each group were separated, and the presence of TNF- $\alpha$ , IL-6, and IL-8 was detected by ELISA, respectively. The remaining cell samples were washed with PBS buffer, and then the total RNA of the cells was extracted using Trizol reagent. After the corresponding cDNA was prepared, PCR amplification was initiated. *GAPDH* was used as an internal reference gene and the relative expression of each group of target genes (*Bax*, *Bcl-2*, *Caspase-3*, *TLR2*, *TLR4*, *MyD88*) was characterized by the 2- $\Delta\Delta$ Ct method (See Table 3).

### Statistical analyses

Every experimental value was reported as means  $\pm$  standard deviation (SD), and group differences were evaluated using one-way analysis of variance (ANOVA). P values less than 0.05 were regarded as significant, and P values less than 0.01 as highly significant.

**Table 3** Primers used in this study

Gene	Forward (5'-3')	Reverse (5'-3')
<i>WalR</i>	TGCTGATGGCCGTAAT	CCAGGTAAGATGGCTTAGAGG
<i>Walk</i>	GATCTTGCCATGCCCCATC	GAGAACGCCGTGAGTTTGTG
<i>StkP</i>	GTTGGGCTCAGTTCAT-TACTTGTCA	CAATAACGGACGGCAGGGGT
<i>PcsB</i>	CAAGCATTGACTACGAAA-CAGGC	TGTTGGACGAACTTTTGCAC-GGA
<i>PspA</i>	CAAAATCCCAATCTCCACA	CCGTATAAAAGGGCTTCAA
<i>LytB</i>	GCAGGGAAAAGTAGTAGAGC-GTT	AAGCCATCCTTAATCCAGACAT
<i>16SrDNA</i>	ACTCCTACGGGAGGCAG-CAGT	TATTACCGCGGTCTGCTGGC
<i>Bax</i>	ACCAAGGTGCCGGAAGTGTAT	AAGATGGTCACGGTCCAACC
<i>Bcl-2</i>	AGGATAACGGAGGCTGGGTA	TTTTATTTCGCCGCTCCAC
<i>Caspase-3</i>	TGGTTTGAGCCTGAGCAGAG	TGGCAGCATCATCCACACAT
<i>TLR2</i>	TCCTGCTAAGAGACTCCTCT-GT	TGGGGAGTGCCCCAAATACT
<i>TLR4</i>	TTCATCATCCAGATTTTC-CAGC	TGTTCCACAGCCTTTCACCT
<i>MyD88</i>	AAGGTGCCATGGTCTTAG-GTG	GGCAGCTAAATGCCTCAACA
<i>GAPDH</i>	TCGGAGTCAACGGATTTGGT	TTCCCGTTCTCAGCCTTGAC

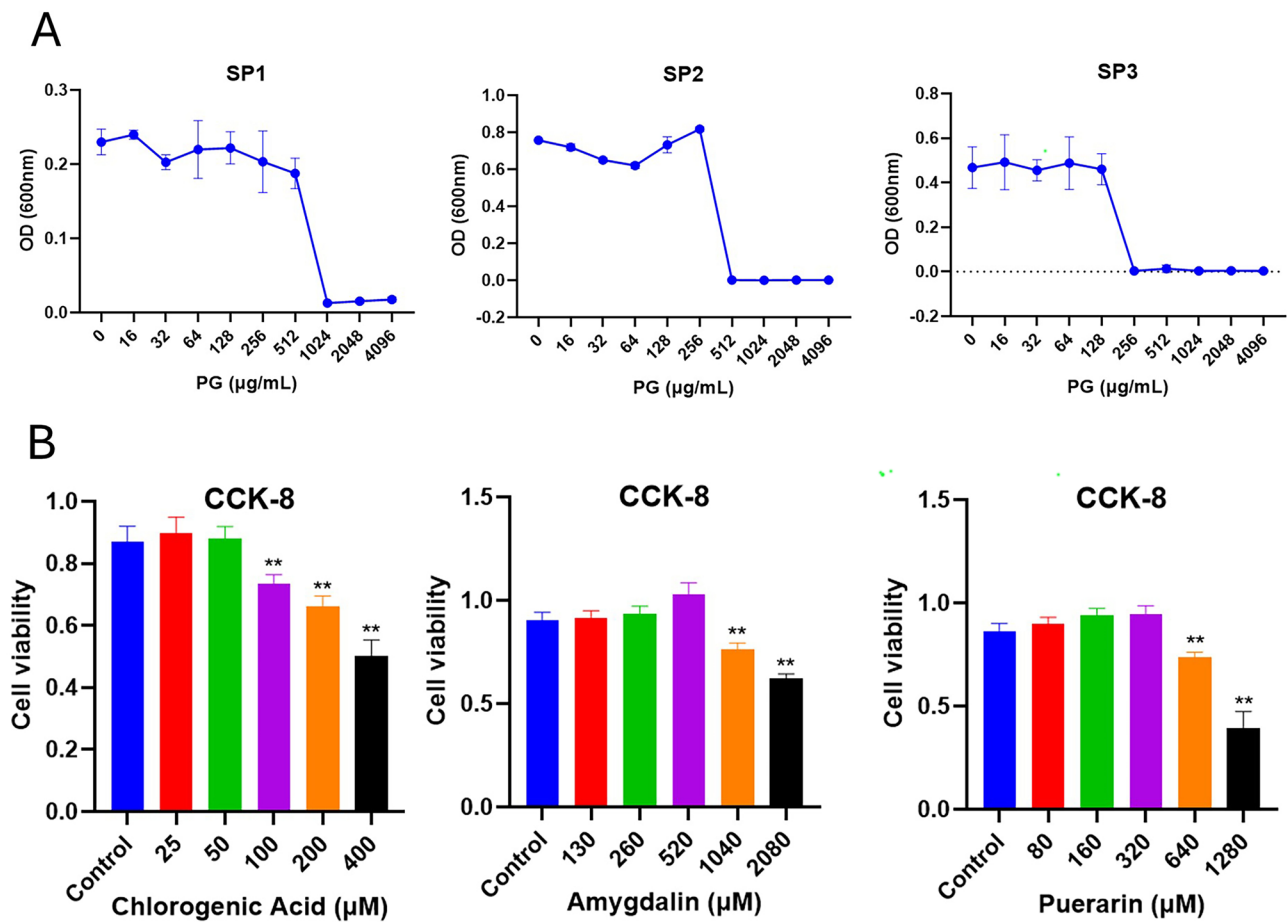


**Fig. 2** Effects of drugs on SP and A549 cells. **(A)** The MICs of PG on SP1, SP2, and SP3 were determined by AST to be 1024, 512, and 256 μg/mL, respectively. **(B)** The TC<sub>50</sub> of C, A, and P on A549 cells were detected by CCK-8 assay to be 50, 520, and 320 μM, respectively. All values are presented as mean ± SD (n = 3). \*\*p < 0.01 vs. control

**Table 4** Analysis of orthogonal design in the bacteriostatic experiment

Group	Chlorogenic acid	Amygdalin	Puerarin	Anti-bacterial rate(%)
1	1	1	1	1.07
2	1	2	2	-1.17
3	1	3	3	0.83
4	2	1	2	3.00
5	2	2	3	-2.27
6	2	3	1	1.67
7	3	1	3	3.07
8	3	2	1	3.43
9	3	3	2	3.83
K in level 1	0.24	2.38	2.06	
K in level 2	0.80	0.00	1.89	
K in level 3	3.44	2.11	0.54	
R	3.20	2.38	1.51	

**Results**

**Optimized combination screened by orthogonal experimental design**

The resistance characteristics of SP strains were analyzed by AST. The resistance of each strain was similar (Fig. 2A), and we selected SP1 as the strain used in the subsequent experiments due to its higher level of resistance to PG (all PRSPs in the subsequent experiments were substituted for SP1).

As shown by the results of the orthogonal analysis of the inhibition experiments (Table 4), it can be seen that the major and minor factors of the active ingredients of YHPG affecting the growth of PRSP were as follows: chlorogenic acid (C) > amygdalin (A) > puerarin (P), and the optimal combination was: A<sub>3</sub>B<sub>1</sub>C<sub>1</sub>, i.e., high-level C (16 μg/mL), low-level A (24 μg/mL), and low-level P (24 μg/mL) had the most apparent tendency to inhibit the growth of PRSP. And the results of the corresponding ANOVA (Table 5) likewise indicated a similar trend. The optimal combination is referred to as CAP (C: 16 μg/mL, A: 24 μg/mL, P: 24 μg/mL).

**Table 5** Variance analysis of orthogonal design in the bacteriostatic experiment

	Sum of squares	df	Mean square	F	Significance
C	17.54	2	8.77	4.38	0.189
A	10.18	2	5.09	2.54	0.282
P	4.12	2	2.06	1.03	0.493
Error	4.00	2	2.00		
Sum	35.84	8			

For the ensuing trials, the experimental groups' dosage regimens were established as follows: PG group (PG:16  $\mu\text{g/mL}$ ), CAP group (C:16  $\mu\text{g/mL}$ , A:24  $\mu\text{g/mL}$ , P:24  $\mu\text{g/mL}$ ), and CAP+PG group (C:16  $\mu\text{g/mL}$ , A:24  $\mu\text{g/mL}$ , P:24  $\mu\text{g/mL}$ ; PG:16  $\mu\text{g/mL}$ ).

### Effects of CAP on PRSP virulence factors

The PRSP capsules were observed by CLSM, and autolysin activity was detected by autolysis induction assay. The effects of CAP or PG intervention did not substantially modify the PRSP capsule when compared with the untreated control (Fig. 3A). The results of the autolysis induction assay (Fig. 3B) showed that Triton X-100 induced the autolysis of PRSP compared to the PBS control, whereas all dosing groups slowed down the degree

of autolysis, with the CAP+PG group having a better-slowing effect than the PG group.

### Effects of CAP on PRSP-induced cell damage

Observing the morphology of A549 cells at MOI of 200:1, 100:1, 50:1, and 30:1 by an inverted microscope, we found that about 50% of A549 cells were damaged at MOI of 100:1 (Fig. 4A). In the literature, 40-60% is usually taken as the range of moderate cell death rate [26], which reflects the pathogenicity of microorganisms and retains enough surviving cells to improve the reproducibility of experiments. The LDH assay findings showed a similar tendency, therefore, the subsequent experiments were performed with MOI of 100:1 conducted. To verify the inhibitory effect of CAP on A549 cell injury, we observed the degree of cell injury with Hoechst/PI staining and LDH levels. The results (Fig. 4B) showed that CAP reduced the mortality of PRSP-infected A549 cells and had a synergistic effect with PG.

Dynamic monitoring of A549 cells by RTCA revealed (Fig. 5) that the intervention of either CAP or PG reduced the death of A549 cells at several time points, 6 h, 12 h, 18 h, and 24 h after PRSP infection of the cells, and the combination of CAP and PG once again showed synergistic effects.

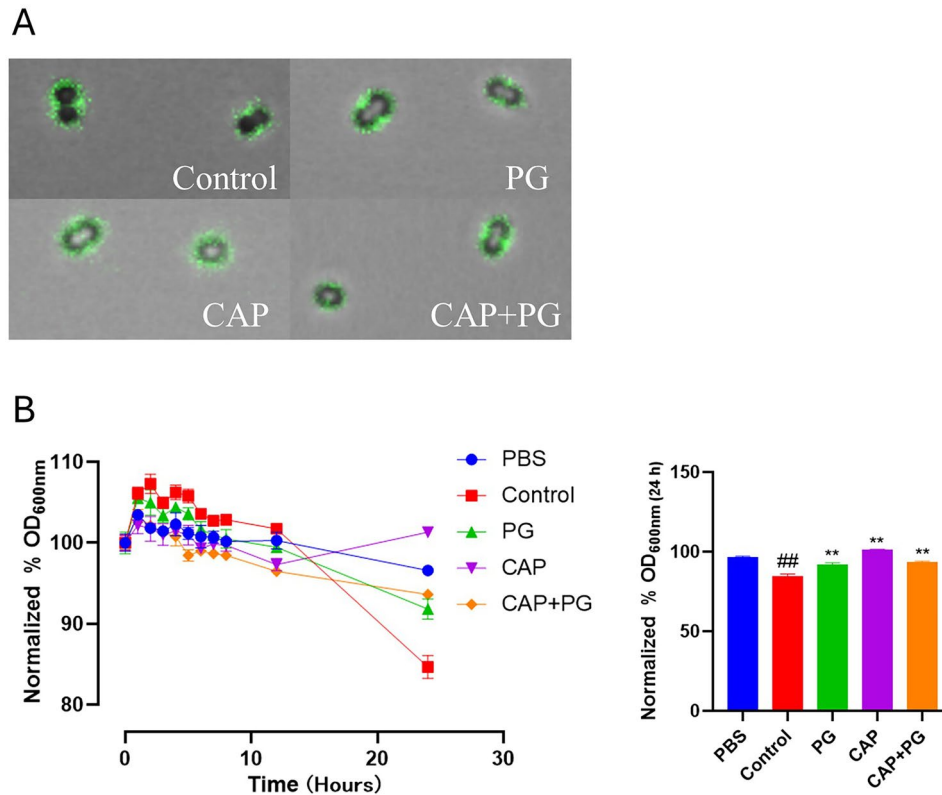


**Fig. 3** CAP had no significant effect on PRSP capsules but reduced PRSP autolysis activity. **(A)** Capsules were treated with FITC-dextran and observed using CLSM. **(B)** Autolysis was induced using Triton X-100 and autolysis activity was evaluated by the amount of change in OD<sub>600</sub>. All values are expressed as mean  $\pm$  SD ( $n=3$ ). ## $p < 0.01$  vs. PBS group; \*\* $p < 0.01$  vs. control

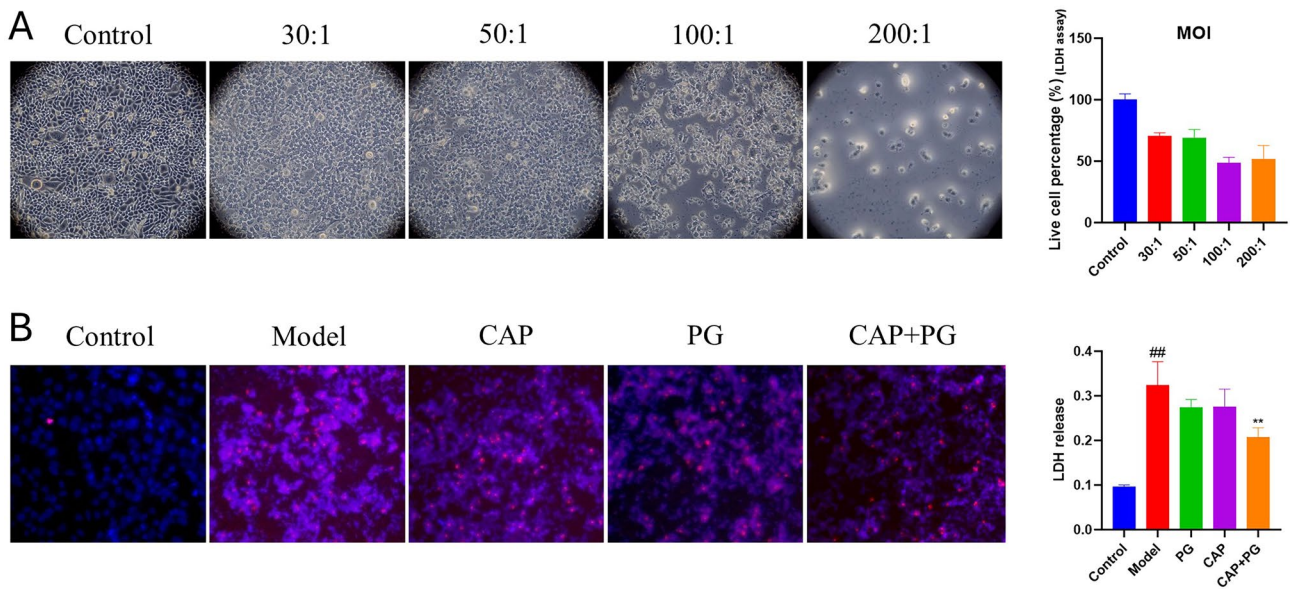


**Fig. 4** 100:1 was the optimal MOI; CAP attenuated PRSP-induced A549 cell damage. **(A)** Effects of various MOIs on A549 cells, cytotoxicity was assessed by microscopic observation (cells in 96-well plates) and LDH assay (cells in 6-well plates), respectively. **(B)** Effects of drugs on A549 cells after PRSP infection as measured by Hoechst 33,342/PI double staining and LDH assay. All values are expressed as mean  $\pm$  SD ( $n=3$ ). ## $p < 0.01$  vs. control; \*\* $p < 0.01$  vs. model

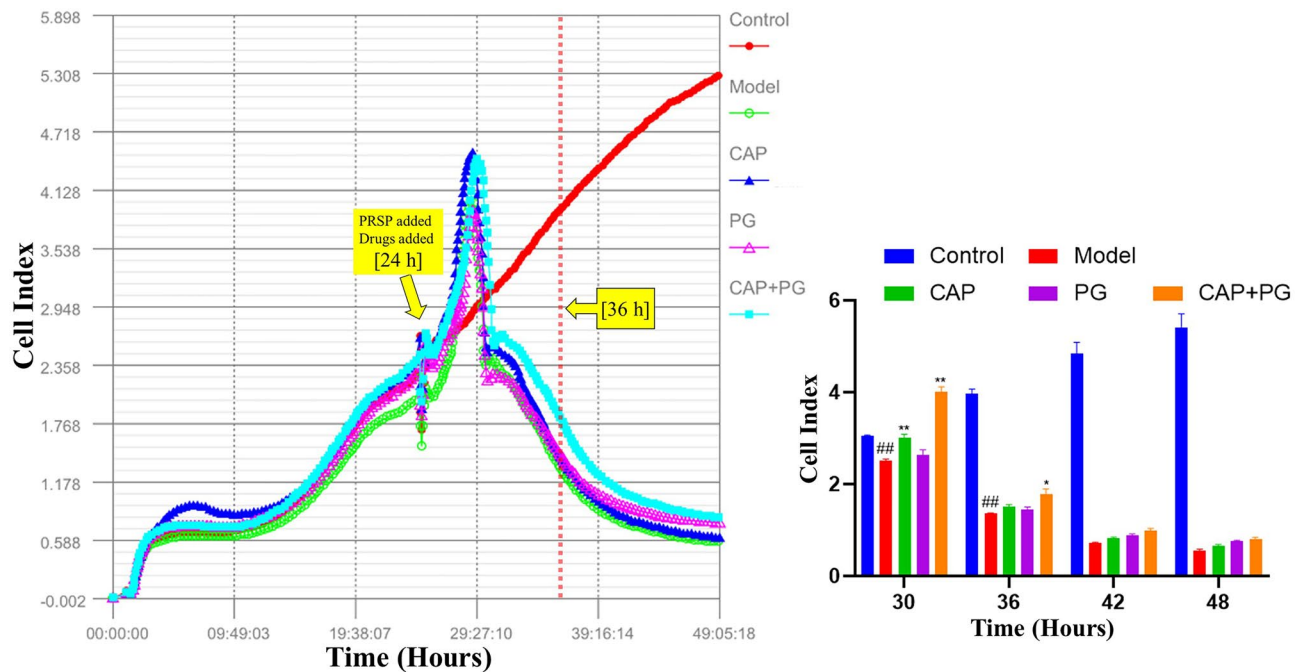


**Fig. 5** CAP promotes the growth status of PRSP-infected A549 cells. Growth of A549 cells was monitored by RTCA. The protective effects of the drugs were also analyzed at specific time points (30 h, 36 h, 42 h, 48 h). The values in the bar graph are expressed as mean  $\pm$  SD ( $n=2$ ). ## $p < 0.01$  vs. control; \* $p < 0.05$ , \*\* $p < 0.01$  vs. model

**Effects of CAP on PRSP-induced apoptosis**

According to the flow cytometry data (Fig. 6A, B), PRSP induction resulted in a significantly higher rate of apoptosis in A549 cells when compared to the control group. However, CAP reversed this trend to some extent, and the combination of CAP and PG may produce more

desirable outcomes than either treatment alone. Furthermore, the mRNA expression levels of *Bax*, *Bcl-2*, and *Caspase-3* genes related to apoptosis/anti-apoptosis were detected by RT-PCR (Fig. 6C). The PRSP group had significantly higher levels of *Bax* and *Caspase-3* than the control group, and correspondingly lower levels of

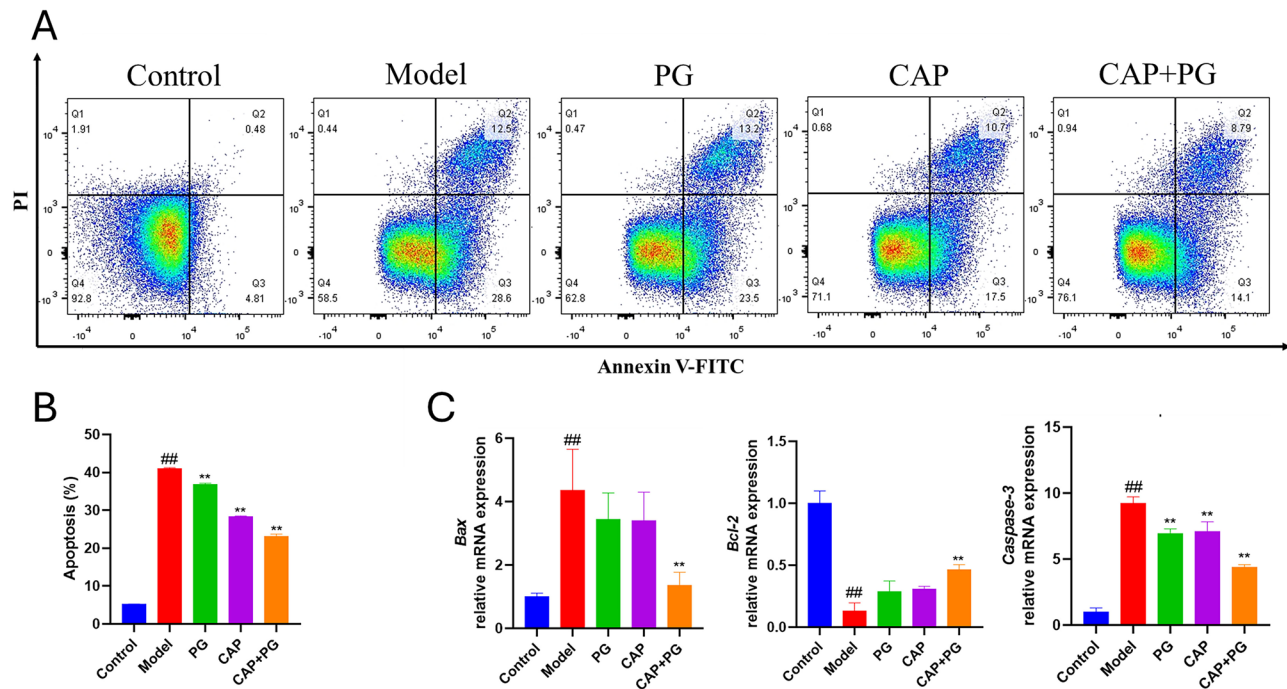


**Fig. 6** CAP attenuates PRSP-induced apoptosis in A549 cells. (A–B) The apoptosis levels were detected by flow cytometry. (C) Relative mRNA expression of *Bax*, *Bcl-2*, and *Caspase-3* was analyzed by RT-qPCR. All values in the bar graphs are expressed as mean ± SD (n = 3). ##p < 0.01 vs. control; \*\*p < 0.01 vs. model

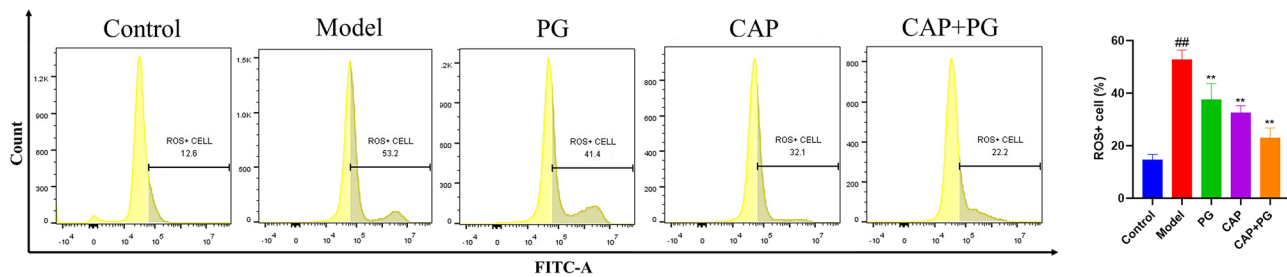


**Fig. 7** CAP reduced PRSP-induced ROS levels in A549 cells. ROS levels were detected by flow cytometry. All values in the bar graphs are expressed as mean ± SD (n = 3). ##p < 0.01 vs. control; \*\*p < 0.01 vs. model

*Bcl-2*. In contrast, the PRSP group had higher levels of *Bcl-2* and lower levels of *Bax* and *Caspase-3* after the CAP interference. In a similar vein, the CAP + PG group outperformed the CAP group in terms of ameliorative effect.

**Effects of CAP on PRSP-induced ROS level**

To verify whether CAP modulates ROS levels in A549 cells after PRSP infection, we assessed ROS levels employing flow cytometry. The addition of PRSP produced a significant elevation of ROS levels in A549 cells, as Fig. 7 illustrates; whereas, the intervention of CAP decreased the ROS levels, indicating CAP’s antioxidant activity.

**Effects of CAP on PRSP adhesion/invasion rates**

The CSH of PRSP after pharmacological intervention was detected by the MATH assay, and the results (Fig. 8A) showed that CAP or its combination with PG decreased the CSH of PRSP, indicating that CAP may lessen PRSP adhesion to A549 cells by lowering PRSP’s CSH. To further investigate, we analyzed the impact of CAP upon PRSP adhesion/invasion towards A549 cells by CFU counting method. The adhesion/invasion rate was lower in all dosage groups as compared to the model group, as evidenced in Fig. 8. Additionally, CAP and PG worked in concert to produce a synergistic effect.

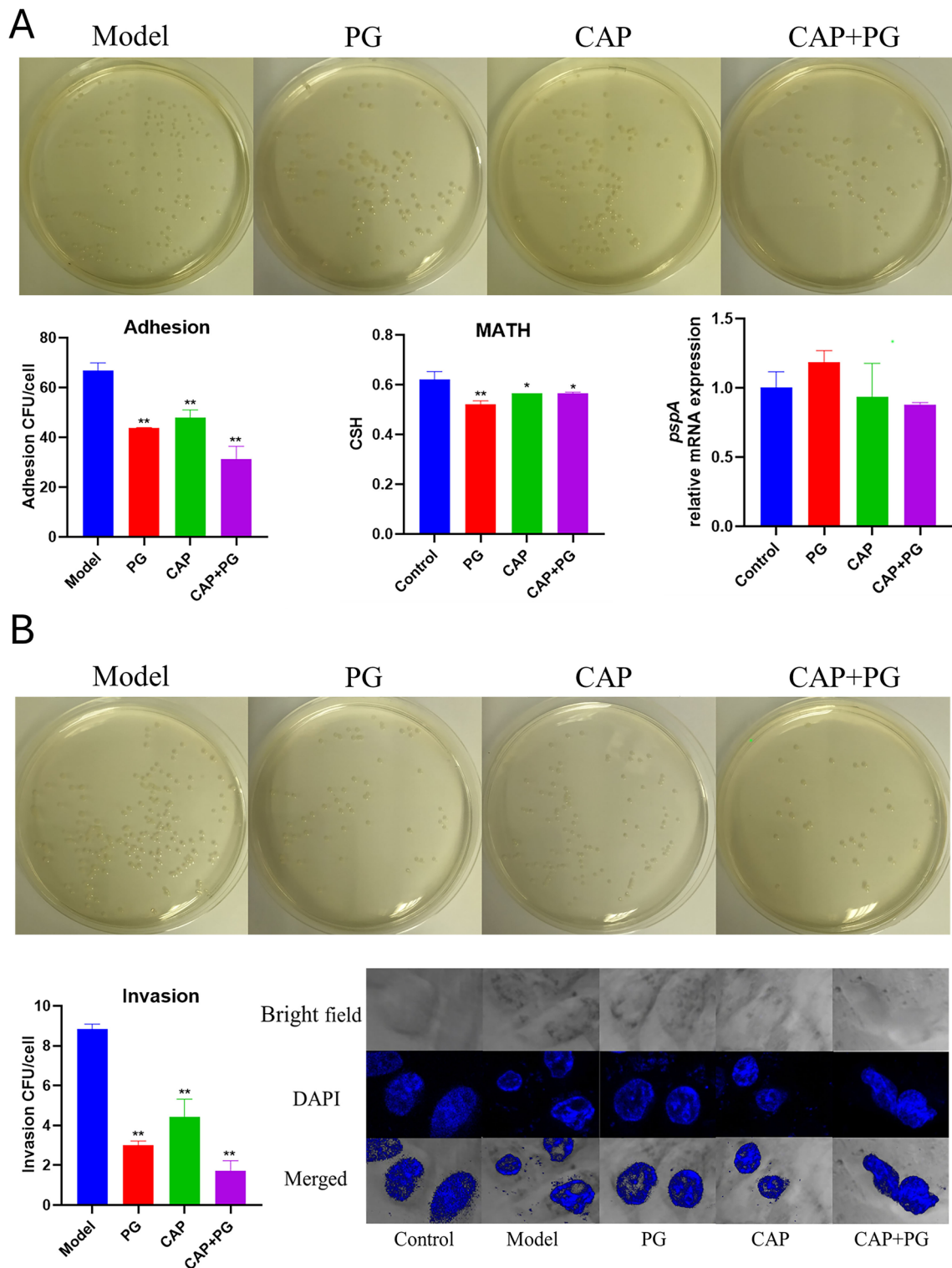


**Fig. 8** CAP reduced the adhesion and invasion rates of PRSP on A549 cells. **(A)** The adhesion ability of PRSP was assessed by adhesion assay, MATH assay and RT-qPCR. **(B)** the invasion status of PRSP was shown by invasion assay and CLSM observation. All values are expressed as mean  $\pm$  SD ( $n=3$ ). \* $p < 0.05$ , \*\* $p < 0.01$  vs. model or control

### Effects of CAP on PRSP-induced inflammatory cytokine secretion

The effect of CAP on PRSP-induced inflammatory cytokine secretion was analyzed by ELISA. Apparently, CAP decreased the release of pro-inflammatory factors TNF- $\alpha$ , IL-6, and IL-8 induced by PRSP (Fig. 9A). This indicates that CAP lessens the inflammatory response of A549 cells when they are infected by PRSP. Due to the anti-inflammatory effect of CAP, to further explore its signaling mechanism, this study used RT-PCR to identify TLR pathway-related genes. The model group had higher levels of each target's expression than the control group (Fig. 9B). *TLR-2*, *TLR-4*, and *MyD88* expression declined substantially following CAP administration. These

findings suggested that CAP suppressed inflammation by inhibiting the expression of TLRs/MyD88.

### Discussion

SP is one of the major bacterial pathogens in humans [27] and often causes community-acquired pneumonia, resulting in high morbidity worldwide. In developed countries, mortality from SP pneumonia can reach 11–40% [28]. When treating SP infections, PG remains the recommended antibiotic [29]. However, antibiotic therapy alone is facing major challenges due to the increasing resistance of isolates [30]. For thousands of years, respiratory infectious disorders have been treated using traditional Chinese medicine [31], which has

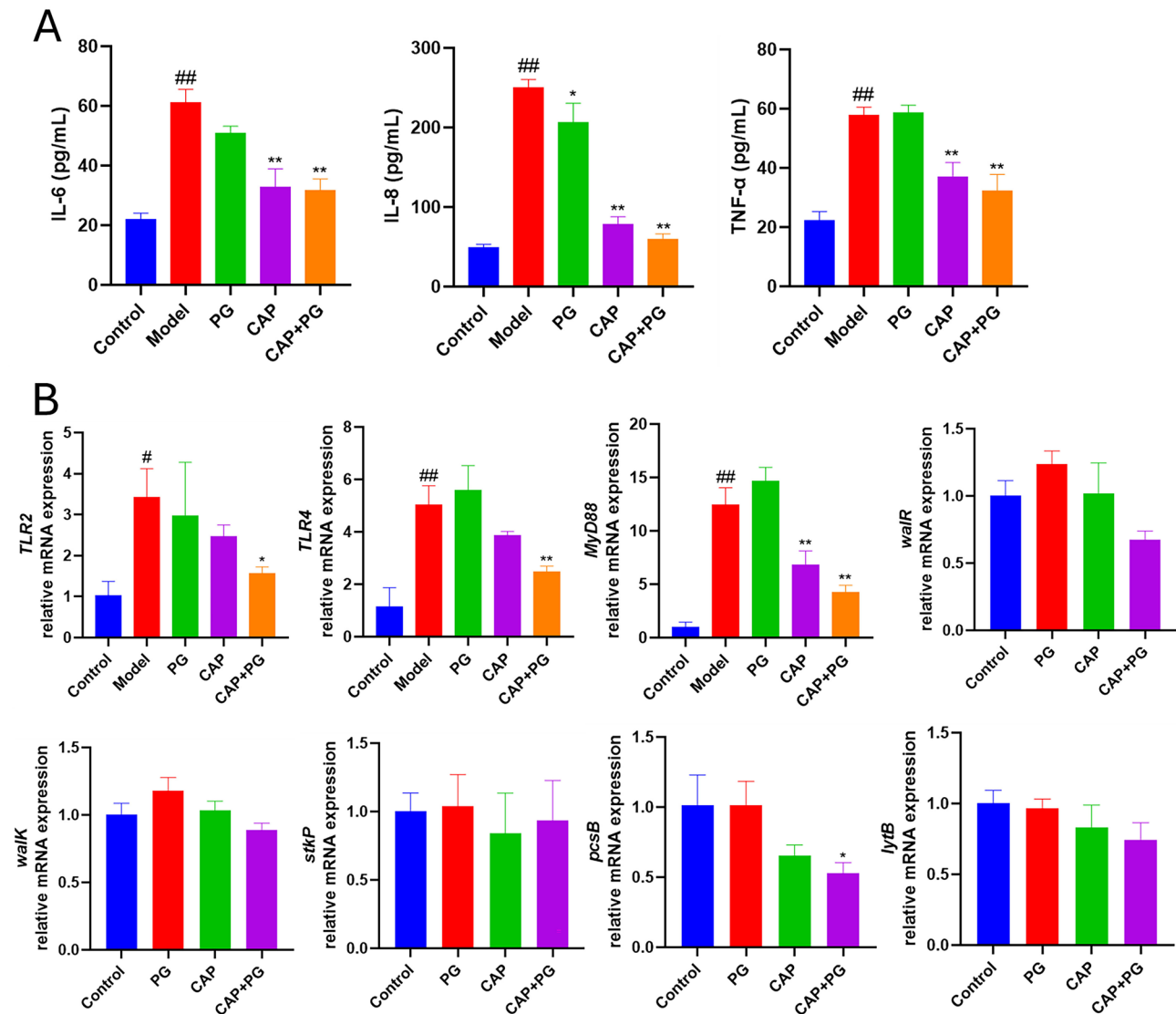


**Fig. 9** CAP attenuates inflammatory cytokine secretion and down-regulates the expression of TLRs/MyD88-related targets in A549 cells, and also tends to down-regulate PRSP WaiRK TCS-related targets. **(A)** TNF- $\alpha$ , IL-6, and IL-8 levels were analyzed by ELISA; **(B)** mRNA expression levels of *TLR2*, *TLR4*, and *MyD88* in A549 cells & *waiR*, *waiK*, *stkP*, *pcsB*, and *lytB* in PRSP were analyzed by RT-qPCR. All values are expressed as mean  $\pm$  SD ( $n=3$ ). # $p < 0.05$ , ## $p < 0.01$  vs. control; \* $p < 0.05$ , \*\* $p < 0.01$  vs. model

shown promising therapeutic results in actual clinical settings. Studies [32–34] have indicated that the naturally occurring compounds C, A, and P possess anti-inflammatory and antioxidant characteristics. We screened an optimized combination of these three main components of YHPG, CAP (C: 16 µg/mL, A: 24 µg/mL, and P: 24 µg/mL), by an orthogonally designed experiment. The present investigation revealed the protective effect of the optimized combination CAP on PRSP-infected A549 cells and the inhibitory effect on PRSP.

When SP is transmitted through the respiratory tract, its capacity to cause infections in the lower respiratory tract is necessary for the development of pneumonia [35], and the bacterial surface changes as a first step [36] in adapting to the pulmonary environment. The primary cause of SP's pathogenicity is the capsule [37]. As the outermost layer of the SP, it protects the bacteria during the invasion into the host cell [38]. Antimicrobial peptides produced by the respiratory epithelium of the host destroy germs on contact. According to recent data, the autolysis of SP counteracts the killing effect of antimicrobial peptides by using its cell wall hydrolase activity [39] to dislodge the capsules [40]. Considering that the capsules of SP belong to a structure with a variable porosity, we observed PRSP under CLSM after incubation with FITC-dextran with reference to the method of Gates MA et al. [41]. The CLSM observation's findings (Fig. 3A) showed that CAP did not have a significant effect on the generation of PRSP capsules. However, results of the autolysis induction assay (Fig. 3B) showed that the intervention of CAP caused a decrease in the autolysin activity of PRSP, suggesting that PRSP has a reduced ability to withstand environmental stresses.

The adhesion and invasion of epithelial cells is the second phase in SP's adaptation to the lung environment [35]. SP exposes more proteins and forms tighter interactions with host cells as they adapt to the lung environment [42]. After SP adheres to lung epithelial cells, it will invade the cells at the appropriate time, albeit less efficiently than invasive bacterial pathogens such as *Salmonella* and *Shigella* [43]. In our experiments (Fig. 8A), the bacterial CSH measured by the MATH method decreased after incubation of PRSP with CAP, while PCR results showed that CAP resulted in the down-regulation of the adhesion-associated protein, PspA, at the transcriptional level, indicating that PRSP's capacity to adhere to the surface of A549 cells was diminished. The results of the adhesion assay (Fig. 8A) verified this. We hypothesized that CAP may have reduced the CSH of the bacterium by regulating the expression of certain adhesion proteins of PRSP, thereby reducing the adhesion rate of PRSP to A549 cells. As for the invasion, the observation of CLSM and the invasion assay (Fig. 8B) showed that CAP decreased the invasion rate of PRSP on A549

cells. Studies [40] showed that the detachment of capsules mediated by the autolytic activity of SP promoted the tight adhesion of SP to host cells and increased the invasion rate of SP on epithelial cells. The decrease in the autolytic activity of PRSP induced by the CAP intervention mentioned above may indirectly lead to a lower rate of PRSP adhesion/invasion to A549 cells. The decrease in PRSP infestation rate, according to Pizarro-Cerdá et al. [44], also implies a decrease in the effective external expression of its virulence.

Following host cell death, host molecules are usually released extracellularly [45], including lactate dehydrogenase (LDH). It is noteworthy that incubation of PspA with host LDH during SP-induced lung inflammation can lead to enhanced virulence of SP and that LDH's enzymatic activity is necessary to increase pneumococcal virulence [46]. Our results (Fig. 4B) showed that CAP reduced PRSP-induced LDH release from A549 cells. This suggests that in the PRSP-induced A549 cell model, CAP not only reduces A549 cytotoxicity but also impairs the overall virulence of PRSP.

SP triggers an inflammatory response in the lungs during the colonization process of continuous adaptation to the pulmonary environment. Severe inflammation is one of the main characteristics of SP illness, and factors such as peptidoglycan, teichoic acid, and pneumolysin (Ply) are able to work together to trigger inflammation through multiple inflammatory cascade responses [47]. Epithelial cells recognize pathogens through PRRs including TLRs for the purpose of signaling to the organism the initiation of the removal of microbial components [48]. For example, TLR2 recognizes cell wall components and TLR4 recognizes Ply [49]. Recognizing these pathogen-associated molecular patterns (PAMPs), TLRs bind to the junction molecules, thereby initiating downstream NF-κB signaling [50]. NF-κB signaling induced by SP infection can serve as the first signal for the induction of NLRP3, while Ply can provide the material basis for the activation of the second signal for the assembly of NLRP3 inflammasome [51]. The ensuing activation of caspase-1 induces the maturation and release of IL-1β and IL-18, which can exacerbate inflammation and tissue damage [52]. It has been demonstrated that the lung epithelium may detect entire bacteria *in vitro* [53] and subsequently release pro-inflammatory cytokines to accelerate the development of pneumonia, such as IL-8 and IL-6 [54]. Our earlier studies [12, 21] showed that YHPG attenuated the inflammatory response by down-regulating the expression of TLR4 and TLR7 and decreasing the levels of pro-inflammatory factors, such as IL-5 and IL-6, in a viral infection model. And according to our study, CAP, the optimized combination of the main components from YHPG, reduced the TNF-α, IL-8, and IL-6 levels in the supernatant during PRSP infection of A549

cells (Fig. 9A) and down-regulated the TLR2, TLR4, and MyD88 expression levels (Fig. 9B), these results further showed the anti-inflammatory function of CAP.

In addition to SP-specific components such as peptidoglycan and Ply, H<sub>2</sub>O<sub>2</sub> produced by SP is one of the determinants of the level of inflammation in the lungs [55]. H<sub>2</sub>O<sub>2</sub> accumulates due to the lack of the H<sub>2</sub>O<sub>2</sub>-degrading enzyme catalase [56], and ROS has also been implicated as a virulence factor in SP. In alveolar epithelial cells exposed to pneumococcal infection, ROS has been demonstrated [57] to cause DNA damage and apoptosis. Applying the flow cytometry investigation (Fig. 7), we noticed that CAP decreased the proportion of ROS<sup>+</sup> cells and apoptotic cells, which reflects the antioxidant effect of CAP.

The parameter CI obtained by RTCA is a multi-dimensional index, which can reflect the characteristics of the quantity, morphology, and size of wall-affixed cells in real time and comprehensively, and make up for the defects of the end-point assay that is not accurate and comprehensive. Notably, in the present study, the RTCA data revealed that during the first 5 h of incubation of PRSP with A549 cells, the CI increased significantly, even forming a sharp “single peak” with respect to the comparison group, which is comparable to that of the *A. baumannii*-induced human respiratory epithelial cell model [58] in an earlier investigation; after reaching the “peak”, the CI of the model and experimental groups decreased rapidly; following that, these groups’ CIs shrank more slowly. We hypothesized that during the early stage of co-culture of PRSP and A549 cells (i.e., the early stage of infection), PRSP continuously adapted to the new environment (e.g., changes in PRSP capsules and autolysin, etc.) and reproduced through binary fission, while A549 cells accelerated their proliferation in response to corresponding stimuli; whereas, when the number of PRSP continuously converged to the threshold, the adhesion/invasion ability of PRSP to lung epithelial cells was continuously enhanced, and CI then decreased rapidly; after that, the change of CI also leveled off, indicating that PRSP and epithelial cells entered the co-existence stage (late stage of infection). In the four time points we examined (Fig. 5), either CAP or PG intervention tended to increase CI, and the synergistic effect of these two resulted in the best improvement in the CAP + PG group. In Fig. 5, 36 h (i.e., after 12 h of co-culture of PRSP and A549 cells) is exactly in the middle of the co-existence phase of PRSP and A549 cells, which best reflects the effect of drug intervention. And the detection points in our study were all after 12 h of co-culture of PRSP with A549 cells, so it can be said that the results of RTCA, not only continuously showed the changes of the bacteria-host cell interactions over a period of time, but also gave direct positive support to

the reliability of the selection of detection time points for our experimental design.

Studies have shown that, unlike the use of antibiotics alone, the combination of herbal components and antibiotics may reduce bacterial resistance to antibiotics [59]. In order to treat SP-induced pneumonia, continuous infusion of PG to maintain its blood concentration at 16–20 µg/mL is generally considered as the optimal “high-dose” regimen [60]. Therefore, the PG concentration was set at 16 µg/mL in this study, and we combined the optimized orthogonal combination with PG. The overall superiority of the combination of antibiotics and herbal components over the usage of each component alone was demonstrated by the findings of our trial. The synergistic effect of CAP and PG may have multiple implications in clinical practice. Firstly, compared with PG alone, CAP can intervene at multiple targets to intervene in bacterial metabolism targets and regulate human immune targets, taking into account the etiology of the disease and the restoration of the body’s function, and promoting the prognosis of PRSP pneumonia. Second, the combination of CAP can reduce the side effects of PG, reduce the dosage can reduce the toxicity of PG [61], especially for children, the elderly, and other sensitive populations. Finally, the use of CAP can improve the efficacy of PG, prolong the service life of PG, and reduce the need to be forced to escalate the use of the last-line antibiotics [62].

We attempted to further investigate the possible reasons for the enhanced bacterial inhibition of herbal components in combination with antibiotics. TCS regulates bacterial oxidative stress, virulence expression, cell wall homeostasis, and energy metabolism [63]. It is the most widely employed mechanism by bacteria to detect and respond to changes in their surroundings [64]. Prior research indicates that upregulation of WalKR TCS can cause increased vancomycin resistance and lead to the development of vancomycin-intermediate *Staphylococcus aureus* (VISA) clinical isolates [65].

PG blocks peptidoglycan biosynthesis by competitively inhibiting the binding of lipid II, the cell wall precursor molecule with a β-lactam structure, to penicillin-binding proteins (PBPs). Blocked lipid II utilization leads to cell wall disruption as well as high levels of lipid II. The serine/threonine protein kinase StkP recognizes β-lactam structures [66] and activates WalK [67] through direct protein-protein interactions. Subsequently, WalR upregulates the expression of enzymes PcsB, LytB, etc. (Fig. 10), required for cell wall remodeling to repair the cell wall [68, 69] and restore cell wall homeostasis. Interestingly, the virulence factor PspA [42] is also regulated by WalR, while LytB is one of the SP autolysins. When SP is sensitive to PG, the repairing ability of SP to the cell wall is weaker than the breaking ability of PG to the cell

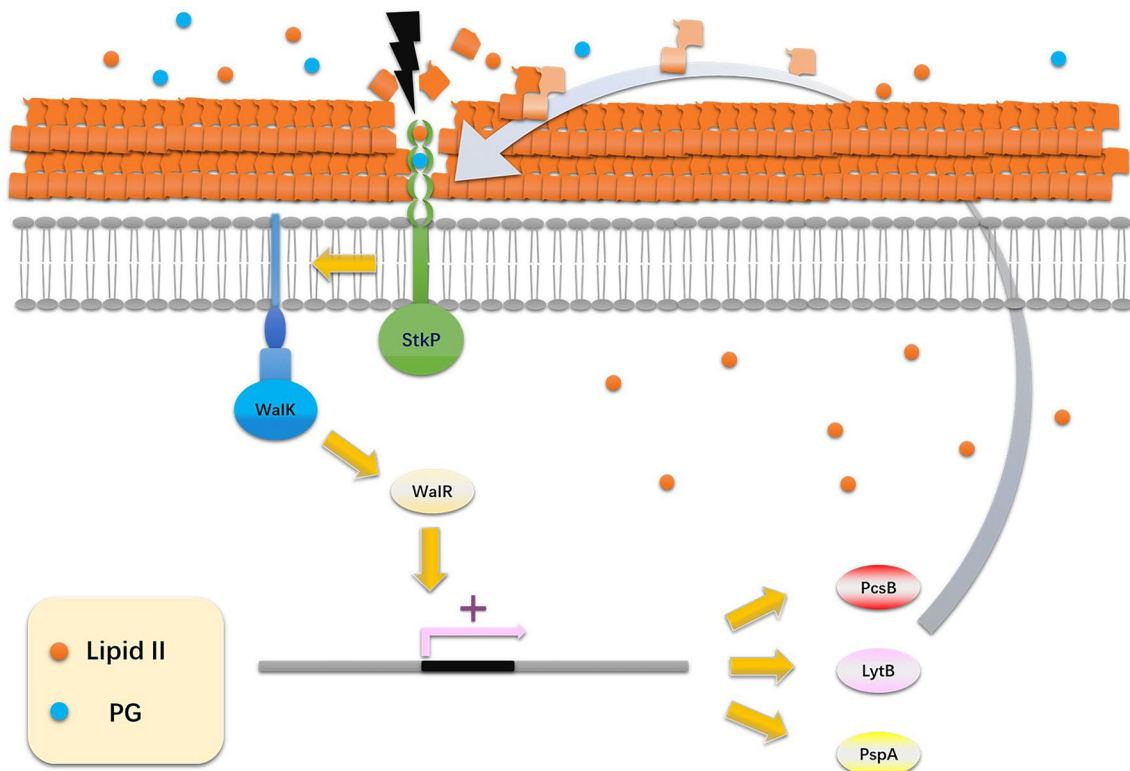


**Fig. 10** WalRK TCS is involved in the maintenance of cell wall homeostasis in *Streptococcus pneumoniae*

wall, and SP growth is inhibited; while when SP is resistant to PG, the repairing ability of SP to the cell wall is stronger than the breaking ability of PG to the cell wall, and the inhibitory effect of PG will be further limited. Our results (Fig. 9B) showed that PcsB was significantly down-regulated under CAP+PG treatment, and there was also a trend of down-regulation of WalR, WalK, LytB, etc. The down-regulation of PcsB suggests that PRSP has a reduced ability to renew or repair the cell wall [70]. We hypothesized that CAP may have weakened PRSP's ability to repair the cell wall by down-regulating WalR/PcsB signaling, resulting in a certain degree of reduced tolerance of PRSP to PG. In other words, the inhibition of the reduced expression of WalRK TCS-related targets by CAP may have reduced the ability of PRSP to maintain cell wall homeostasis, thereby increasing the sensitivity of PRSP to PG to some extent.

This study combines traditional Chinese medicine with modern biological techniques to show the dual potential of CAP in reducing bacterial virulence and host inflammation, as with its synergistic effect with PG. However, this study still has some limitations. For example, although GA can inhibit PRSP-induced inflammatory responses, it has not been further investigated at the dimensions of NF- $\kappa$ B, MAPKs, and NLRP3. In addition, this study focused on in vitro cellular models, and future pharmacokinetic and in vivo validation of CAP is needed.

## Conclusion

In summary, we found that the optimized combination of CAP had protective effects on PRSP-infected A549 cells. On the one hand, the protective effect of CAP was through inhibiting the virulence of PRSP; on the other hand, CAP attenuated the inflammatory response by inhibiting the TLRs/MyD88 pathway and the release of pro-inflammatory cytokines, which attenuated cellular damage. In addition, the synergistic effect of CAP with PG may be due to the fact that CAP reduced the drug resistance of PRSP by inhibiting WalRK TCS. These findings are consistent with the multi-target and multi-pathway characteristics of herbal components and offer fresh concepts and approaches for the clinical management of diseases caused by PRSP infection.

## Abbreviations

A	Amygdalin
AST	Antibiotic susceptibility test
C	Chlorogenic acid
CLSM	Confocal laser scanning microscope
CSH	Cell-surface hydrophobicity
ELISA	Enzyme-linked immunosorbent assay
MATH	Microbial adhesion to hydrocarbon
MOI	Multiplicity of infection
P	Puerarin
PAMP	Pathogen-associated molecular patterns
PBPs	Penicillin-binding proteins
PG	Penicillin G
Ply	Pneumolysin
PRR	Pattern recognition receptor

PRSP	Penicillin-resistant <i>Streptococcus pneumoniae</i>
ROS	Reactive oxygen species
RTCA	Real time cellular analysis
TCS	Two-component regulatory system
TCO	Maximal atoxic concentration
TLRs	Toll-like receptors
VISA	Vancomycin-intermediate <i>Staphylococcus aureus</i>
YHPG	Yinhuapinggan granules

### Acknowledgements

We are grateful to the authors for their unreserved support for the smooth progress of this study.

### Author contributions

Jiangbo Lv: Writing—review and editing, Writing—original draft, Validation, Methodology, Investigation, Formal analysis, Data curation, Conceptualization. Haofang Wan: Writing—review and editing, Supervision, Project administration. Daojun Yu: Writing—review and editing, Visualization, Validation, Supervision, Formal analysis, Data curation. Huifen Zhou: Validation, Supervision. Wenba Wang: Visualization, Validation. Haitong Wan: Writing—review and editing, Supervision, Software, Resources, Funding acquisition, Conceptualization. All authors reviewed the manuscript.

### Funding

This work was financially supported by the Key projects of the National Natural Science Foundation of China 'Study on the effect and mechanism of Qingjie Xuantou Feiwei Decoction (Yinhua Pinggan Granules) and its components on the severity of drug-resistant bacterial pneumonia (project number 81930111).

### Data availability

The raw data supporting the conclusion of this article will be made available by the authors, without undue reservation.

### Declarations

#### Ethics approval and consent to participate

Not applicable.

#### Consent for publication

Not applicable.

#### Competing interests

The authors declare no competing interests.

#### Author details

<sup>1</sup>College of Chinese Medicine for Cardiovascular-Cranial Disease, Zhejiang Chinese Medical University, Hangzhou, China

<sup>2</sup>Zhejiang Key Laboratory of Chinese Medicine for Cardiovascular and Cerebrovascular Disease, Hangzhou, China

<sup>3</sup>Hangzhou First People's Hospital, Hangzhou, China

<sup>4</sup>Academy of Chinese Medical Sciences, Henan University of Chinese Medicine, Zhengzhou, Henan Province 450046, China

Received: 9 January 2025 / Accepted: 9 April 2025

Published online: 20 April 2025

### References

- Ali MQ, Kohler TP, Schulig L, Burchhardt G, Hammerschmidt S. Pneumococcal extracellular Serine proteases: molecular analysis and impact on colonization and disease. *Front Cell Infect Microbiol*. 2021;11:763152.
- GBD 2016 Lower Respiratory Infections Collaborators. Estimates of the global, regional, and National morbidity, mortality, and aetiologies of lower respiratory infections in 195 countries, 1990–2016: a systematic analysis for the global burden of disease study 2016. *Lancet Infect Dis*. 2018;18(11):1191–210.
- Kalitzang'oma A, Chaguza C, Gori A, Davison C, Beleza S, Antonio M, et al. *Streptococcus pneumoniae* serotypes that frequently colonise the human nasopharynx are common recipients of penicillin-binding protein gene fragments from *Streptococcus mitis*. *Microb Genom*. 2021;7(9):000622.
- Subramanian K, Banerjee A, Editorial. Deceiving the host: mechanisms of immune evasion and survival by Pneumococcal bacteria. *Front Cell Infect Microbiol*. 2023;13:1231253.
- World Health Organization. WHO publishes list of bacteria for which new antibiotics are urgently needed. Available at: <https://www.who.int/news-room/detail/27-02-2017-who-publishes-list-of-bacteria-for-which-new-antibiotic-s-are-urgently-needed>
- Subramanian K, Henriques-Normark B, Normark S. Emerging concepts in the pathogenesis of the *Streptococcus pneumoniae*: from nasopharyngeal colonizer to intracellular pathogen. *Cell Microbiol*. 2019;21(11):e13077.
- Johnson BK, Abramovitch RB. Small molecules that sabotage bacterial virulence. *Trends Pharmacol Sci*. 2017;38(4):339–62.
- Chen X, Luo W, Gao Q, Chen C, Li L, Liu D, et al. Incorporating Single-Copper sites and host defense peptides into a nanoreactor for antibacterial therapy by bioinspired design. *Engineering*. 2024;43(12):216–27.
- Butler MS, Paterson DL. Antibiotics in the clinical pipeline in October 2019. *J Antibiot (Tokyo)*. 2020;73(6):329–64.
- Dai C, Liu Y, Lv F, Cheng P, Qu S. An alternative approach to combat multidrug-resistant bacteria: new insights into traditional Chinese medicine monomers combined with antibiotics. *Adv Biotechnol (Singap)*. 2025;3(1):6.
- Guan S, Zhu K, Dong Y, Li H, Yang S, Wang S, et al. Exploration of binding mechanism of a potential *Streptococcus pneumoniae* neuraminidase inhibitor from herbaceous plants by molecular simulation. *Int J Mol Sci*. 2022;21(3):1003.
- Chen T, Du H, Zhou H, Yang J, Zhu J, Tong X, et al. Screening of antiviral components of Yinhuapinggan granule and protective effects of Yinhuapinggan granule on MDCK cells with influenza A/H1N1 virus. *Biomed Res Int*. 2022;2022:1040129.
- Guo T, Guo Y, Liu Q, Xu Y, Wei L, Wang Z, et al. The TCM prescription Ma-xing-shi-gan-tang inhibits *Streptococcus pneumoniae* pathogenesis by targeting Pneumolysin. *J Ethnopharmacol*. 2021;275:114133.
- Wang Y, Wang X, Li Y, Xue Z, Shao R, Li L, et al. Xuanfei Baidu Decoction reduces acute lung injury by regulating infiltration of neutrophils and macrophages via PD-1/IL17A pathway. *Pharmacol Res*. 2022;176:106083.
- Peng XQ, Zhou HF, Lu YY, Chen JK, Wan HT, Zhang YY. Protective effects of Yinhuapinggan granule on mice with influenza viral pneumonia. *Int Immunopharmacol*. 2016;30:85–93.
- He Y, Yu D, Zhang Y, Yang J, Zhou H, Wan H. Anti-tussive effect experiment of Yinhua Pinggan granule. *Chin Archives Traditional Chin Med*. 2014;32(09):2060–1.
- Chen T, Du H, Zhou H, He Y, Yang J, Li C, et al. Yinhuapinggan granule ameliorates lung injury caused by multidrug-resistant *Acinetobacter baumannii* via inhibiting NF- $\kappa$ B/NLRP3 pathway. *Heliyon*. 2023;9(11):e21871.
- Mukherjee S, Patra R, Behzadi P, Masotti A, Paolini A, Sarshar M. Toll-like receptor-guided therapeutic intervention of human cancers: molecular and immunological perspectives. *Front Immunol*. 2023;14:1244345.
- Behzadi P, Sameer AS, Nissar S, Banday MZ, Gajdacs M, Garcia-Perdomo HA, et al. The Interleukin-1 (IL-1) superfamily cytokines and their single nucleotide polymorphisms (SNPs). *J Immunol Res*. 2022;2022:2054431.
- Behzadi P, Chandran D, Chakraborty C, Bhattacharya M, Saikumar G, Dhama K, et al. The dual role of toll-like receptors in COVID-19: balancing protective immunity and Immunopathogenesis. *Int J Biol Macromol*. 2025;284(Pt 2):137836.
- Peng XQ, Zhou HF, Zhang YY, Yang JH, Wan HT, He Y. Antiviral effects of Yinhuapinggan granule against influenza virus infection in the ICR mice model. *J Nat Med*. 2016;70(1):75–88.
- Song J, Zhang F, Tang S, Liu X, Gao Y, Lu P, et al. A module analysis approach to investigate molecular mechanism of TCM formula: A trial on Shu-feng-jie-du formula. *Evid Based Complement Alternat Med*. 2013;2013:731370.
- Liu BG, Xie M, Dong Y, Wu H, He DD, Hu GZ, et al. Antimicrobial mechanisms of traditional Chinese medicine and reversal of drug resistance: a narrative review. *Eur Rev Med Pharmacol Sci*. 2022;26(15):5553–61.
- Liu Y, Zhang M, Cai Y, Wu S, Mei C, Wang H, et al. Synergistic antimicrobial efficacy of glabrol and colistin through micelle-based co-delivery against multidrug-resistant bacterial pathogens. *Phytomedicine*. 2025;137:156371.
- Bacova J, Knotek P, Kopecka K, Hromadko L, Capek J, Nyvltova P, et al. Evaluating the use of TiO2 nanoparticles for toxicity testing in pulmonary A549 cells. *Int J Nanomed*. 2022;17:4211–25.
- Wen SH, Lin LN, Wu HJ, Yu L, Lin L, Zhu LL, et al. TNF- $\alpha$  increases *Staphylococcus aureus*-induced death of human alveolar epithelial cell line A549 associated with RIP3-mediated necroptosis. *Life Sci*. 2018;195:81–6.

27. Wantuch PL, Avci FY. Current status and future directions of invasive Pneumococcal diseases and prophylactic approaches to control them. *Hum Vaccin Immunother*. 2018;14(9):2303–9.
28. Daniels CC, Rogers PD, Shelton CM. A review of Pneumococcal vaccines: current polysaccharide vaccine recommendations and future protein antigens. *J Pediatr Pharmacol Ther*. 2016;21(1):27–35.
29. von Specht M, García Gabarrot G, Mollerach M, Bonofiglio L, Galetti P, Kaufman S, et al. Resistance to  $\beta$ -lactams in *Streptococcus pneumoniae*. *Rev Argent Microbiol*. 2021;53(3):266–71.
30. Antimicrobial Resistance Collaborators. Global burden of bacterial antimicrobial resistance in 2019: a systematic analysis. *Lancet*. 2022;399(10325):629–55.
31. Chang JS, Yeh CF, Wang KC, Shieh DE, Yen MH, Chiang LC. Xiao-Qing-Long-Tang (Sho-seiryu-to) inhibited cytopathic effect of human respiratory syncytial virus in cell lines of human respiratory tract. *J Ethnopharmacol*. 2013;147(2):481–7.
32. Zhang X, Huang H, Yang T, Ye Y, Shan J, Yin Z, et al. Chlorogenic acid protects mice against lipopolysaccharide-induced acute lung injury. *Injury*. 2010;41(7):746–52.
33. Barakat H, Aljuttaily T, Almujaydil MS, Algheshairy RM, Alhomaïd RM, Almutairi AS, et al. Amygdalin: A review on its characteristics, antioxidant potential, Gastrointestinal microbiota intervention, anticancer therapeutic and mechanisms, toxicity, and encapsulation. *Biomolecules*. 2022;12(10):1514.
34. Zhou YX, Zhang H, Peng C. Puerarin: a review of Pharmacological effects. *Phytother Res*. 2013;28(7):961–75.
35. Loughran AJ, Orihuela CJ, Tuomanen EI. *Streptococcus pneumoniae*: invasion and inflammation. *Microbiol Spectr*. 2019;7(2). <https://doi.org/10.1128/microbiolspec.GPP3-0004-2018>.
36. Kahya HF, Andrew PW, Yesilkaya H. Deacetylation of Sialic acid by esterases potentiates Pneumococcal neuraminidase activity for mucin utilization, colonization and virulence. *PLoS Pathog*. 2017;13(3):e1006263.
37. Dao TH, Rosch JW. JMM profile: *Streptococcus pneumoniae*: sugar-coated captain of the men of death. *J Med Microbiol*. 2021;70(11):001446.
38. Nakamoto R, Banyaci S, Blomqvist K, Normark S, Henriques-Normark B, Sham LT. The divisome but not the elongasome organizes capsule synthesis in *Streptococcus pneumoniae*. *Nat Commun*. 2023;14(1):3170.
39. Ramos-Sevillano E, Urzainqui A, Campuzano S, Moscoso M, González-Camacho F, Domenech M, et al. Pleiotropic effects of cell wall amidase LytA on *Streptococcus pneumoniae* sensitivity to the host immune response. *Infect Immun*. 2015;83(2):591–603.
40. Kietzman CC, Gao G, Mann B, Myers L, Tuomanen EI. Dynamic capsule restructuring by the main Pneumococcal autolysin LytA in response to the epithelium. *Nat Commun*. 2016;7:10859.
41. Werren JP, Mostacci N, Gjuroski I, Holivilolona L, Troxler LJ, Hathaway LJ, et al. Carbon source-dependent capsule thickness regulation in *Streptococcus pneumoniae*. *Front Cell Infect Microbiol*. 2023;13:1279119.
42. Gómez-Mejía A, Gámez G, Hammerschmidt S. *Streptococcus pneumoniae* two-component regulatory systems: the interplay of the Pneumococcus with its environment. *Int J Med Microbiol*. 2018;308(6):722–37.
43. Cundell DR, Gerard NP, Gerard C, Idanpaan-Heikkilä I, Tuomanen EI. *Streptococcus pneumoniae* anchor to activated human cells by the receptor for platelet-activating factor. *Nature*. 1995;377(6548):435–8.
44. Pizarro-Cerdá J, Cossart P. Bacterial adhesion and entry into host cells. *Cell*. 2006;124(4):715–27.
45. Gonzalez-Juarbe N, Bradley KM, Riegler AN, Reyes LF, Brissac T, Park SS, et al. Bacterial Pore-Forming toxins promote the activation of caspases in parallel to necroptosis to enhance alarmin release and inflammation during pneumonia. *Sci Rep*. 2018;8(1):5846.
46. Park SS, Gonzalez-Juarbe N, Martínez E, Hale JY, Lin YH, Huffines JT, et al. *Streptococcus pneumoniae* binds to host lactate dehydrogenase via PspA and PspC to enhance virulence. *mBio*. 2021;12(3):e00673–21.
47. Tomasz A, Saukkonen K. The nature of cell wall-derived inflammatory components of Pneumococci. *Pediatr Infect Dis J*. 1989;8(12):902–3.
48. Zaiful Anuar NF, Mohd Desa MN, Hussaini J, Wong EH, Mariappan V, Vellamy KM, et al. Role of cell surface proteins and toll-like receptors in the pathogenesis of *Streptococcus pneumoniae*. *Iran J Basic Med Sci*. 2024;27(2):214–22.
49. Loh LN, Gao G, Tuomanen EI. Dissecting bacterial cell wall entry and signaling in eukaryotic cells: an Actin-Dependent pathway parallels Platelet-Activating factor Receptor-Mediated endocytosis. *mBio*. 2017;8(1):e02030–16.
50. Kawai T, Ikegawa M, Ori D, Akira S. Decoding Toll-like receptors: recent insights and perspectives in innate immunity. *Immunity*. 2024;57(4):649–73.
51. LaRock CN, Nizet V. Inflammasome/IL-1 $\beta$  responses to Streptococcal pathogens. *Front Immunol*. 2015;6:518.
52. Xu J, Núñez G. The NLRP3 inflammasome: activation and regulation. *Trends Biochem Sci*. 2023;48(4):331–44.
53. Sorrentino R, de Souza PM, Srisukandan S, Duffin C, Paul-Clark MJ, Mitchell JA. Pattern recognition receptors and interleukin-8 mediate effects of Gram-positive and Gram-negative bacteria on lung epithelial cell function. *Br J Pharmacol*. 2008;154(4):864–71.
54. Watanabe N, Yokoe S, Ogata Y, Sato S, Imai K. Exposure to *Porphyromonas gingivalis* induces production of Proinflammatory cytokine via TLR2 from human respiratory epithelial cells. *J Clin Med*. 2020;9(11):3433.
55. Feldman C, Anderson R, Cockeran R, Mitchell T, Cole P, Wilson R. The effects of Pneumolysin and hydrogen peroxide, alone and in combination, on human ciliated epithelium in vitro. *Respir Med*. 2002;96(8):580–5.
56. Klabunde B, Wesener A, Bertrams W, Ringshandl S, Halder LD, Vollmeister E, et al. *Streptococcus pneumoniae* disrupts the structure of the golgi apparatus and subsequent epithelial cytokine response in an H2O2-dependent manner. *Cell Commun Signal*. 2023;21(1):208.
57. Rai P, Parrish M, Tay IJ, Li N, Ackerman S, He F, et al. *Streptococcus pneumoniae* secretes hydrogen peroxide leading to DNA damage and apoptosis in lung cells. *Proc Natl Acad Sci USA*. 2015;112(26):E3421–30.
58. Chen Y, Shao T, Fang S, Pan P, Jiang J, Cheng T, et al. Effect of calcium on the interaction of *Acinetobacter baumannii* with human respiratory epithelial cells. *BMC Microbiol*. 2019;19(1):264.
59. Wang J, Lu X, Wang C, Yue Y, Wei B, Zhang H, et al. Research progress on the combination of Quorum-Sensing inhibitors and antibiotics against bacterial resistance. *Molecules*. 2024;29(7):1674.
60. Bryan CS, Talwani R, Stinson MS. Penicillin dosing for Pneumococcal pneumonia. *Chest*. 1997;112(6):1657–64.
61. Doña I, Guidolin L, Bogas G, Olivieri E, Labella M, Schiappoli M, et al. Resensitization in suspected penicillin allergy. *Allergy*. 2023;78(1):214–24.
62. Walia K, Sharma M, Vijay S, Shome BR. Understanding policy dilemmas around antibiotic use in food animals & offering potential solutions. *Indian J Med Res*. 2019;149(2):107–18.
63. Diagne AM, Pelletier A, Durmort C, Faure A, Kanonenberg K, Freton C, et al. Identification of a two-component regulatory system involved in antimicrobial peptide resistance in *Streptococcus pneumoniae*. *PLoS Pathog*. 2022;18(4):e1010458.
64. Yu WL, Pan JG, Qin RX, Lu ZH, Bai XH, Sun Y. TCS01 Two-Component system influenced the virulence of *Streptococcus pneumoniae* by regulating PcpA. *Infect Immun*. 2023;91(5):e0010023.
65. Dubrac S, Bisicchia P, Devine KM, Msadek T. A matter of life and death: cell wall homeostasis and the walk (YycGF) essential signal transduction pathway. *Mol Microbiol*. 2008;70(6):1307–22.
66. Maestro B, Nováková L, Heseck D, Lee M, Leyva E, Mobashery S, et al. Recognition of peptidoglycan and  $\beta$ -lactam antibiotics by the extracellular domain of the Ser/Thr protein kinase StkP from *Streptococcus pneumoniae*. *FEBS Lett*. 2011;585(2):357–63.
67. Stamsås GA, Straume D, Salehian Z, Håvarstein LS. Evidence that Pneumococcal walk is regulated by StkP through protein-protein interaction. *Microbiol (Reading)*. 2017;163(3):383–99.
68. Sasková L, Nováková L, Basler M, Branny P. Eukaryotic-type serine/threonine protein kinase StkP is a global regulator of gene expression in *Streptococcus pneumoniae*. *J Bacteriol*. 2007;189(11):4168–79.
69. Fleurie A, Manuse S, Zhao C, Campo N, Cluzel C, Lavergne JP, et al. Interplay of the serine/threonine-kinase StkP and the paralogs diviva and GpsB in Pneumococcal cell elongation and division. *PLoS Genet*. 2014;10(4):e1004275.
70. Sham LT, Barendt SM, Kopecky KE, Winkler ME. Essential PcsB putative peptidoglycan hydrolase interacts with the essential FtsXSpn cell division protein in *Streptococcus pneumoniae* D39. *Proc Natl Acad Sci U S A*. 2011;108(45):E1061–9.

## Publisher's note

Springer Nature remains neutral with regard to jurisdictional claims in published maps and institutional affiliations.